ELSA/4-2012-BGO

Proposal to the PAC

Vector Meson Photoproduction at BGO-OD

The BGO-OD Collaboration

Spokesperson: H. Schmieden, P. Levi Sandri
Contact Person: V. Vegna and J. Hannappel
e-mail: vegna@physik.uni-bonn.de; hannappel@physik.uni-bonn.de

B. Bantes [1], D. Bayadilov [2], R. Beck [2], M. Becker [2], A. Bella [1], J. Bieling [1], S. Boese [2], A. Braghieri [3], K. Brinkmann [4], D. Burdeynyi [5], F. Curciarello [6,7], V. De Leo [6,7], R. Di Salvo [8], H. Dutz [1], D. Elsner [1], A. Fantini [8,9], T. Frese [1], F. Frommberger [1], V. Ganenko [5], G. Gervino [10,18], F. Ghio [11,12], G. Giardina [6,7], B. Girolami [11,12], D. Glazier [13], S. Goertz [1], A. Gridnev [14], D. Hammann [1], J. Hannappel [1], W. Hillert [1], A. Ignatov [15], O. Jahn [1], R. Jahn [2], R. Joosten [2], T.C. Jude [1], F. Klein [1], K. Koop [2], B. Krusche [16], A. Lapik [15], P. Levi Sandri [17], I. Lopatin [14], G. Mandaglio [6,7], F. Messi [1], R. Messi [8,9], D. Moricciani [8], V. Nedorezov [15], D. Noviskiy [14], P. Pedroni [3], M. Romaniuk [6,7], T. Rostomyan [16], C. Schaerf [8,9], H. Schmieden [1], V. Sumachev [14], V. Tarakanov [14], V. Vegna [1], P. Vlasov [2], D. Walther [2], D. Watts [13], H.-G. Zaunick [2], T. Zimmermann [1]

[1] Physikalisches Institut, Nussallee 12, D-53115 Bonn
[2] Helmholtz-Institut fr Strahlen- und Kernphysik, Nussallee 14-16, D-53115 Bonn
[3] INFN, Sezione di Pavia, via Agostino Bassi 6, 27100 Pavia, Italy
[4] Justus-Liebig-Universitt Gieen, II. Physikalisches Institut, Heinrich-Buff-Ring 16, D 35392 Gieen
[5] National Science Center Kharkov Institute of Physics and Technology, Akademicheskaya St. 1, Kharkov, 61108, Ukraine
[6] Dipartimento di Fisica e di Scienze della Terra, Università di Messina, v.le F. Stagno d'Alcontres 31, 98166 Messina, Italy
[7] INFN, Sezione di Catania, via Santa Sofia 64, 95123 Catania, Italy
[8] INFN, Sezione di Roma "Tor Vergata", Via della Ricerca Scientifica 1, 00133 Roma, Italy
[9] Dipartimento di Fisica, Università di Roma "Tor Vergata", via della Ricerca Scientifica 1, 00133 Roma, Italy
[10] Dipartimento di Fisica, Università di Torino, via P. Giuria 1, 10125 Torino, Italy
[11] INFN, Sezione di Roma, c/o Dipartimento di Fisica - Università di Roma "La Sapienza", P.le Aldo Moro 2, 00185 Roma, Italy
[12] Istituto Superiore di Sanità, viale Regina Elena 299, 00161 Roma, Italy
[13] The University of Edinburgh, James Clerk Maxwell Building, Mayfield Road, Edinburgh EH9 3JZ UK
[14] Petersburg Nuclear Physics Institute, Gatchina, Leningrad District, 188300 Russia
[15] Russian Academy of Sciences Institute for Nuclear Research, prospekt 60-letiya Oktyabrya 7a, Moscow 117312 Russia
[16] Institut fr Physik, Klingelbergstrasse 82, CH-4056 Basel
[17] INFN - LNF, Via E. Fermi 40, 00044 Frascati (Roma), Italy
[18] INFN, Sezione di Torino, via P. Giuria 1, 10125 Torino, Italy

Bonn, November 5, 2012

Abstract

ω and ϕ meson photoproduction will be investigated with the aim of a simoultanoues study of the dominant t channel exchange contribution (by measuring differential cross sections and spin density matrix elements) and of intermediate resonant states (by measuring beam asymmetries). The polarisation measurements must be extended at least up to 1.8 GeV of incoming photon beam energy, to cover a still unexploited energy region for ω beam asymmetry (previous measurements reach 1.5 GeV) and to access the ϕ channel (which threshold is 1.57 GeV). The detection of final state particles from ω and ϕ decays requires to use a set-up optimised for charged particles detection in the whole transfer momentum t range. We propose to perform this measurements using the BGO-OD set-up at ELSA, which completely fulfills the experimental requirements.

Equipment

All the proposed experiments will be performed using the BGO-OD set-up at the ELSA accelerator. For all of them, the unpolarised electron beam at 3.2 GeV is required. Unpolarised and polarised photon beams will be produced with a Cu and a diamond radiator, respectively. Targets of liquid H_2 and liquid D_2 will be used.

Accelerator & target specification

e^- beam:	3.2 GeV e^- unpolarized
beam line:	BGO-OD experimental area
beam intensity:	10^7 tagged photons/s in the energy range 0.32 - 2.88 GeV
polarization:	unpolarised and linearly polarised (at 1.2, 1.6, 1.7 and 1.8 GeV)
target:	LH_2 and LD_2
trigger:	energy deposited in the BGO calorimeter: > 100 MeV .

beamtime request

LH_2target:	unpolarised	**500 h**
LH_2target:	polarised at 1.2 GeV	**350 h**
LH_2target:	polarised at 1.6 GeV	**350 h**
LH_2target:	polarised at 1.7 GeV	**250 h**
LH_2target:	polarised at 1.8 GeV	**300 h**
LD_2target:	unpolarised	**1000 h**
LD_2target:	polarised at 1.2 GeV	**250 h**
LD_2target:	polarised at 1.6 GeV	**350 h**
LD_2target:	polarised at 1.8 GeV	**450 h**

Contents

List of Figures

List of Tables

1 Introduction

The study of vector meson photoproduction off nucleon is a powerful tool to access information about the internal structure of the nucleon and - more in general - about the features of the strong interaction in the low energy region. Vector meson photoproduction is known to be dominated by t-channel exchange in the low transfer momentum t regime. Contributions from s and u- channels are almost negligible at low t but they could become appreciable at higer t. Therefore, a complete study of vector meson photoproduction off nucleon requires the investigation and understanding of both t-channel exchange terms and intermediate resonant state contributions.
The lightest vector meson (ρ, ω and ϕ) experimental cross sections are shown in Fig.1.
ρ photoproduction is the reaction having the higher cross section. Neverthless, ω and ϕ mesons have much smaller full widths (Γ_ρ = 149.1 $\pm$ 0.8 MeV, while Γ_ω = 8.49 $\pm$ 0.12 MeV and Γ_ϕ = 4.26 $\pm$ 0.04 [1]) which allow for a better signal over background discrimination. Due to this, in the following we will focus only on ω and ϕ photoproduction.
This document is organized as it follows. In section 2 we present the theoretical motivations which

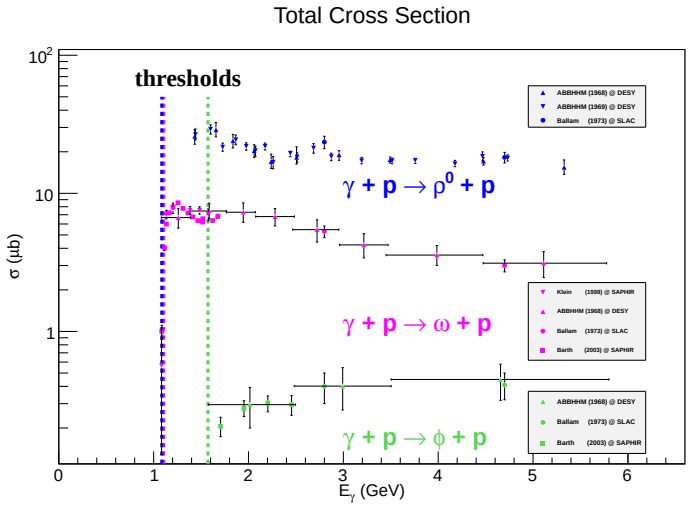

Figure 1 Experimental total cross section of ρ^0 (blue), ω (light purple) and ϕ (green) photoproduction off proton from the corresponding thresholds up to 6 GeV of incoming photon energy. Data for ρ^0 photoproduction are from references [2] (blue triangles), [3] (inverse blue triangles) and [4] (blue circles). Data for ω photoproduction are from references [2] (light purple triangles), [4] (light purple circles), [5] (inverse light purple triangles) and [6] (light purple squares). Data for ϕ photoproduction are from references [2] (green triangles), [4] (green circles) and [7] (full squares).

guided us to propose new experiments on ω photoproduction. In section 2.1 we will discuss the reason why the BGO-OD setup at ELSA is the best suited experiment to performe the desired measurements. The theoretical motivations underlying the proposed ϕ experiments will be discussed in section 3. In section 3.1 it will be explained why we want to carry out these experiments at the BGO-OD experiment.
A brief descritpion of the BGO-OD experimental set-up will be given in section 4.
The request of beam hours for ω experiments consists of a first general discussion about kinematics studies (including geometrical acceptance and detector efficiency) and of a further minimal requirement of beam hours for each measurement (beam asymmetry off proton in section 5.1, spin density matrix elements in section 5.2, differential cross section off proton in section 5.3 and beam asymmetry off neutron in section 5.4).
The request of beam hours for ϕ experiments is organized in the same way: firstly kinematics studies (including geometrical acceptance and detection efficiency) are described and then the minimal requirement of beam hours is given in section 6.1 for the measurement of the differential cross section off proton; in section 6.2 for the beam asymmetry off proton; in section 6.3 for the differential cross section off neutron.
All the information will be summarised in section 7.

2 Theoretical Motivations: ω photoproduction

The ω meson has mass M_ω = 782.65 $\pm$ 0.12 MeV and quantum numbers $I^G(J^{PC}) = 0^-(1^{--})$ [1]. Its main decay modes are listed in Tab.1 with their branching ratios. In Fig.2 differential cross sections of ω photoproduction off proton are shown as a function of the transfer momentum t from threshold (E_γ^{th} =1.1 GeV) up to 4.7 GeV incoming photon energies. The differential cross section shows the typical *diffractive behavior* dropping down with increasing t. This behavior is ascribed to the t-channel exchange terms (namely, Pomeron and pseudo-scalar meson), which are the dominant contributions of the production at low t. For higher t values and with increasing energy the description of the differential cross section requires the introduction of direct and crossed nucleon terms in s and u-channel and of resonant term contributions. A recent publication from CLAS Collaboration [9] provides high-statistics results both for the differential cross section and for the spin density matrix elements for the reaction $\gamma p \to \omega p$ (with unpolarised photon beam). The interpretation of the results [10] requires the inclusion of contributions from $F_{15}(1680)$ and $D_{13}(1700)$ intermediate resonant states at threshold and underlines the evidence for additional contributions from resonant states with mass W = 1.8 - 2.0 GeV. Since ω has isospin I=0, only N^* resonant states can contribute to the production process.

decay mode	B.R. (%)
$\pi^+\pi^0\pi^-$	89.2 ± 0.7
$\pi^0\gamma$	8.28 ± 0.28
$\pi^+\pi^-$	$1.53\ ^{+0.11}_{-0.13}$

Table 1 Main ω decay modes [1]

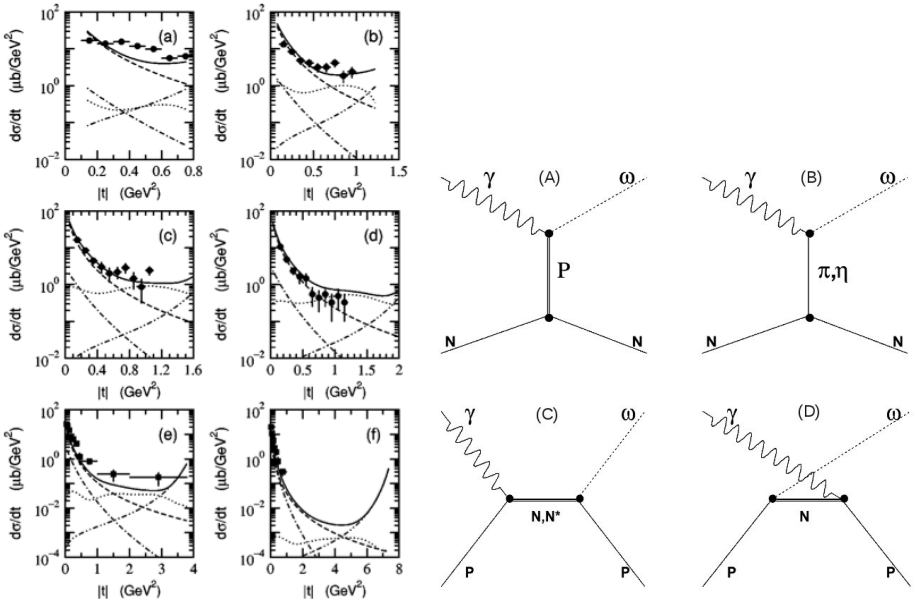

Figure 2 **Left panel.** Differential cross section of ω photoproduction off free proton as a function of the transfer momentum t at several incoming photon beam energy: (a) E_γ = 1.23 GeV; (b) E_γ = 1.45 GeV; (c) E_γ = 1.68 GeV; (d) E_γ = 1.92 GeV; (e) E_γ = 2.8 GeV; (f) E_γ = 4.7 GeV; (FIG.2 from Ref.[8]). Data from Ref. [4] (full squares) and [5] (full circles) are described by the model in Ref.[8] including: Pomeron exchange in the t-channel (dot-dashed line), pseudoscalar meson exchange (dashed line), direct and crossed term in s and u channel (dot-dot-dashed line) and N^* excitation (dotted line). The total amplitude is given by solid line. **Right panel.** Diagrams corresponding to the main production terms: (A) Pomeron exchange in the t-channel; (B) pseudoscalar meson exchange in the t-channel; (C) Born term and resonant contribution in the s-channel; (D) cross term in the u-channel.

The best way to access information about resonant state contributions consists in the measurement of polarization observables and, in particular, of the photon beam asymmetry Σ. It has been shown that Σ is expected to be null if only non resonant terms contribute to the production process. Any deviation from the null behavior is a signature of s-channel resonance contributions. Already published results

of Σ for the reaction $\vec{\gamma}p \rightarrow \omega p$ are shown in Fig.3 (left panel). Data cover the energy range from threshold (E_γ = 1.1 GeV) up to 1.5 GeV corresponding to a center of mass energy range W = 1.72 - 1.92 GeV. Green squares results are from GRAAL Collaboration [11] and black stars points are from CBELSAT/TAPS Collaboration [12]. In the first case, the ω meson has been identified by the three-pion decay ($\omega \rightarrow \pi^+\pi^0\pi^-$); in the latter case, by the radiative decay ($\omega \rightarrow \pi^0\gamma$). In both cases, an important deviation from the null behavior is observed, confirming the important contribution of resonant states in the ω production process. The two results are not in agreement within the errors and they show different angular distributions. In particular, important differences are observed at θ^*_ω = 60° in two over the four energy bins, since a fast rise is observed in CBELSA/TAPS results which is totally absent in GRAAL data. Moreover, for highest θ^*_ω values GRAAL results always show null asymmetry while CBELSA/TAPS results show still negative asymmetries in three bins over four. In the right panel of Fig.3 descriptions of Σ are shown for several models. It is evident that the descriptions are still strongly model dependent and that new measurements are urgently required to assest the status of beam asymmetry measurement. In addiction, results from CLAS underline the importance of extending Σ measurement to the center of mass energy W =1.8 - 2.0 GeV (corresponding to incoming photon beam energies up to 1.8 GeV) to verify the contribution of resonant states introduced to better describe the differential cross section behavior.

In parallel, the study of t-channel exchange terms is necessary for a complete understanding of ω photoproduction. The measurement of the spin-density matrix elements is necessary to estimate the relative contributions of natural (for example, Pomeron) and unnatural (for example, π^0 and η) parity exchange terms in the t-channel and to better understand the intrinsic polarization of the ω meson itself. This can be performed by measuring the angular distributions of the ω decay products. High statistics data for unpolarised spin density matrix elements (ρ^0_{00}, ρ^0_{1-1} and $Re(\rho^0_{10})$) have been published by CLAS [9]. Results of spin density matrix elements from linearly polarised photoproduction (ρ^1_{00}, ρ^1_{1-1} and $Re(\rho^1_{10})$) are still not available in literature.

The further step in the understading of the ω photoproduction process is necessarly the study off neutron target. At present, no results for ω photoproduction off neutron are present in literature. Preliminary results from GRAAL [17] show significant differences between the Σ behavior for the reaction off quasi-free proton and the off quasi-free neutron in D_2 target.

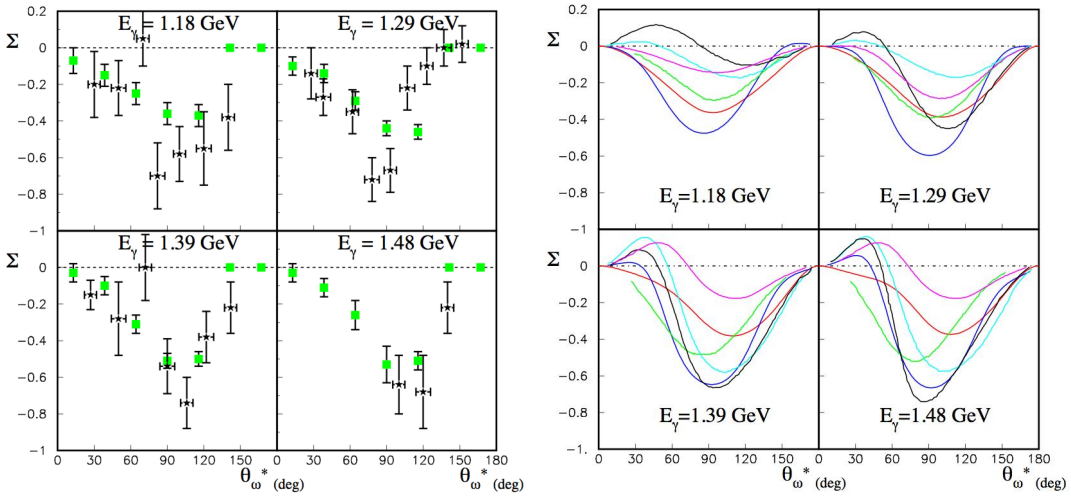

Figure 3 **Left panel** Experimental results of Σ for the reaction $\vec{\gamma}p \rightarrow \omega p$. Data points: green squares from Ref.[11]; black stars from Ref.[12]. **Right panel** Description of Σ for the reaction $\vec{\gamma}p \rightarrow \omega p$ from several theoretical models. Black line and light blue line from [13]; light purple line from [14]; red line from [15]; green line from [12]; blue line from [16].

2.1 ω photoproduction at BGO-OD

According to what has been discussed in the previous section, we want to perform the following measurements for ω photoproduction:

- measurement of the beam asymmetry (Σ in the following) for the reaction $\vec{\gamma}p \rightarrow \omega p$ from threshold up to E_γ = 1.8 GeV (corresponding to the center of mass energy W = 2.06 GeV) investigating both the three-pion decay (having the highest branching ratio B.R. = 89.2 %) and the radiative decay as a cross check on the stability of the results;
- measurement of the spin density matrix elements (SDME's in the following) for the reaction $\vec{\gamma}p \rightarrow \omega p$ with linearly polarised photons from threshold up to E_γ = 1.8 GeV (corresponding to the center of mass energy W = 2.06 GeV), identifying the ω meson by its three-pion decay from very low t-region, where t-channel contribution is the dominant term;
- measurement of the unpolarised differential cross section for the reaction $\gamma n \rightarrow \omega n$ from very low t-region;
- measurement of Σ for the reaction $\vec{\gamma}n \rightarrow \omega n$ investigating both the three-pion decay (having the highest branching ration B.R. = 89.2 %) and the radiative decay as a cross check on the stability of the results.

The BGO-OD experiment at ELSA fulfills all the experimental requirements necessary to performe these measurements since:

1. the ELSA facility provides an electron beam at 3.2 GeV. It allows to produce linearly polarised photon beams by Bremsstrahlung, with significant polarisation degree up to $E_{\vec{\gamma}}$ = 1.8 GeV.
2. the BGO-OD detector is optimized both for multi-charged-particle final states and for multi-photon final states. It allows for the identification of the ω meson by the three-pion decay mode which is characterized by a very high branching ratio (89.2%). This strongly reduces the amount of hours necessary to collect sufficient statistics. The detection of photons from the radiative decay by the BGO detector allows for the cross check of final results.
3. the BGO-OD detector covers the polar angular range θ^{lab} = 2° - 155 ° (with a complete symmetry in the azimuthal angle φ) allowing for measurements at very low transfer momentum t which is the most important region for SDME's extraction and for the measurement of the differential cross section off neutron.

The proposed experiments can not be performed at A2 - MAMI (due to limitation in energy of the photon beam) neither at CB - ELSA, whose detector is not optimized for charged particle detection.

3 Theoretical Motivations: ϕ photoproduction

The ϕ meson has mass M_ϕ = 1019.455 $\pm$ 0.020 MeV and quantum numbers $I^G(J^{PC}) = 0^-(1^{--})$ [1]. Its main decay modes are listed in Tab.3 with their branching ratios.

decay mode	B.R. (%)
K^+K^-	48.9 $\pm$ 0.5
$K^0_L K^0_S$	34.2 $\pm$ 0.4
$\rho\pi + \pi^+\pi^0\pi^-$	15.32 $\pm$ 0.32
$\eta\gamma$	1.309 $\pm$ 0.024

Table 2 Main ϕ decay modes [1]

Measurements from SAPHIR [7] and LEPS collaboration [18] of the differential cross section of the reaction $\gamma p \rightarrow \phi p$ as a function of the transfer momentum t show the dominance of t channel exchange process in ϕ photoproduction. The extrapolation of the differential cross section at the minimum allowed transfer momentum t_{min} is shown in Fig.4. LEPS results (full circles) show a bump structure at $E_\gamma \simeq$ 2.0 GeV which is completely unexpected. The extraction of SDME's from the measured angular distributions of ϕ decay products ($\phi \rightarrow K^+K^-$) confirms the dominant role of the Pomeron exchange term and allows to evaluate as small but not negligible the contribution of the unnatural parity exchange term. The angular distribution of the decay products does not show any dependence on E_γ and no possible origin of the bump structure in Fig.4 has been found. No theoretical model including only t-channel exchanges contributions is able to describe the bump structure. A new independent measurement of the differential cross section at $t = t_{min}$ must be performed to verify the anomalous non monotonic behavior observed by LEPS.
A. Kiswandhi et al [20] found that the introduction of a resonant state (having mass W = 2.10 GeV and total angular momentum J=3/2) could allow for a good description of LEPS results (Fig.5 - left panel) and for a better interpretation of CLAS results of ω differential cross section at W = 2.1 GeV (published in [9]). If resonant terms are really involved in the photoproduction of ϕ off proton, their contribution must be visible in polarisation observables and especially in the beam asymmetry Σ. In Fig.5 (right panel) predictions of this model for polarisation observables at E_γ = 2.0 GeV are given for non-resonant contributions (dotted line), resonant contribution with negative parity (solid line) and resonant contribution with positive parity (dot dashed line). At present, no result of Σ for ϕ photoproduction is present in literature.
The measurement of the differential cross section of ϕ photoproduction off neutron must be performed and then compared with results off proton for a better understanding of the origin of the bump structure shown in Fig.4.

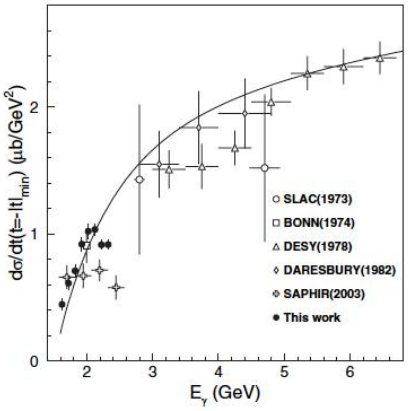

Figure 4 Differential cross section extrapolated at the minimum allowed transfer momentum t_{min} (Fig.5 from Ref.[18]). LEPS data (full circles) show an unexpected bump around 2 GeV of incoming photon energy. The solid curve represents the prediction of a model by Titov [19] including Pomeron trajectory and π and η exchange terms.

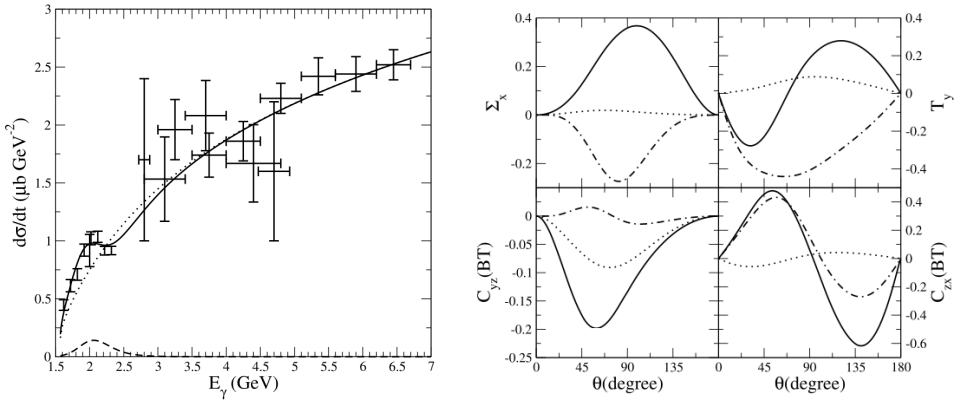

Figure 5 **Left panel.** Description of the differential cross section results by the model in reference [20]. If only t channel exchange contributions are taken into account, the expected behavior of the differential cross section at $t = t_{min}$ is expected to be monotonic (dotted line).If the contribution of an intermediate resonant state (having mass W = 2.1 GeV, $J^P = 3/2^-$ is included (dashed line), the full amplitude (solide line) nicely describes the experimental results. **Right panel.** Description of some polarisation observables by the model in Ref.[20]. Dotted line: only Pomeron and pseudo-scalar meson exchange contribution; dot-dashed line: inclusion of the contribution of a $J^P = 3/2^+$ resonant state (W = 2.1 GeV); solid line: inclusion of the contribution of a $J^P = 3/2^-$ resonant state (W = 2.1 GeV).

3.1 ϕ photoproduction at BGO-OD

The observation of the unexpected non monotonic behavior of the differential cross section by LEPS requires further investigation, since its origin is still unknown. For this motivation, we want to perform the following measurements for ϕ photoproduction:

- new measurement of $d\sigma/dt$ for the reaction $\gamma p \to \phi p$ for comparison with LEPS results, identifying the ϕ meson by the decay $\phi \to K^+K^-$.
- first measurement of Σ for the reaction $\vec{\gamma}p \to \phi p$ to evaluate if only t channel exchange terms must be taken into account or if also resonant contributions must be considered.
- measurement of $d\sigma/dt$ for the reaction $\gamma n \to \phi n$ from threshold (E_γ^{th} = 1.57 GeV up to at least E_γ = 2.3 GeV, i.e. in the same energy range where to the anomalous bump for the proton target has been observed. An extended measurement up to E_γ = 2.8 GeV is desirable.

The BGO-OD experiment at ELSA is the only one (LEPS apart) where these measurements can be performed at small transfer momentum t. The detection of K^+ and K^- from ϕ decay in the polar angular range from 2° to 155° allows to exploit a much wider kinematical region than the one accessible at LEPS and to perform also measurements at high transfer momentum (which are of special importance for Σ).

4 BGO-OD set-up

The BGG-OD detector setup is a combination of a central detector system and a forward spectrometer for charged particles, completed by a photon tagging system.

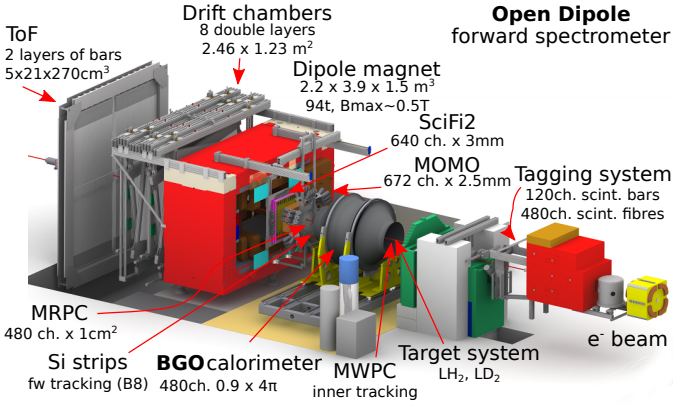

Figure 6 The BGO-OD experimental setup

The central detector of the experimental setup is the high resolution and large solid angle ($0.9 \cdot 4\pi$) BGO[a] electromagnetic calorimeter of the former GRAAL experiment [21, 22, 23, 24]. The calorimeter is combined with two multi-wire proportional chambers (MWPC) for inner tracking and a plastic scintillator barrel for particle identification through the measurement of dE/dx. The calorimeter consists of 480 BGO crystals with a length of 24cm (> 21 radiation lengths).

The region between the acceptance of the central detector and the forward spectrometer will be covered by an azimuthally symmetric Multi-gap Resistive Plate Chamber (MRPC), which is a contribution from external BGO-OD collaborators (INFN Rome and University of Rome). The MRPC will be located between the BGO calorimeter and the MOMO detector. It consists of two stacks, which are divided into 16 independent azimuthal sectors with a total of 480 channels.

The forward spectrometer is based on a large open dipole magnet, a permanent loan by DESY. Tracks are reconstructed in front of the magnet by two fiber hodoscopes, MOMO and SciFi2.

Behind the magnet tracking is done using a set of 8 double layer drift chambers in four different orientations, vertical wires to measure the x-coordinate, horizontal for the y-coordinate, and tilted by $\pm 9^\circ$ from vertical, for a u- and v-coordinate.

The forward spectrometer is completed by a set of time-of-flight walls that are used to discriminate the various particles.

The photon tagging system, uses a series of 120 adjacent, partially overlapping plastic scintillators with fast photomultiplier readout. It is designed to cover an electron energy range between 10% and 90% of the ELSA energy. In 2013 an additional scintillating fiber hodoscope will be added to allow for precise determination of the degree of polarisation for linearly polarized photons by measuring the shape of the coherent edge and increasing energy resolution for low photon energies.

Part	Acceptance	angular resolution	time resolution	p/E resolution
BGO Ball	$25^\circ < \Theta < 155^\circ$	$\Delta\Theta < 6^\circ$,$\Delta\Phi < 7^\circ$	< 3 ns	$\approx 3\,\%$ for 1 GeV photons
MWPC	$18^\circ < \Theta < 163^\circ$	$\Delta\Theta \approx 1^\circ$,$\Delta\Phi = 2^\circ$	n.a.	n.a.
MRPC	$8^\circ < \Theta < 25^\circ$	$< 1^\circ$	50 ps	n.a.
forward spec.	$\Theta_{vert} < 8^\circ$	$\Delta\Theta_{\Theta<4^\circ} < 0.2^\circ$	n.a.	$< 3\,\%$ for $p < 1.5$ GeV
	$\Theta_{hor} < 12^\circ$	$\Delta\Theta_{\Theta<10^\circ} < 0.3^\circ$	n.a.	$< 6\,\%$ for $p < 3$ GeV
ToF	$\Theta_{vert} < 8^\circ$,$\Theta_{hor} < 12^\circ$		500 ps	n.a.
Tagger	n.a.	n.a.	275 ps	10 MeV to 40 MeV

Table 3 Parameters of the BGO-OD setup

[a] $Bi_4Ge_3O_{12}$

5 Request of beamtime: ω photoproduction

The calculation of the necessary beam hours requires the knowledge on the number of ω per second we will be able to collect. This number is calculated according with the following formula:

$$\frac{N_\omega}{s} = \frac{N_\gamma}{s} \cdot N_{SC} \cdot \langle \frac{d\sigma}{d\Omega} \rangle \Delta\Omega \cdot \varepsilon \cdot B.R. \quad (1)$$

with

- $\frac{N_\gamma}{s}$ is the tagged photon flux
- N_{SC} is the number of scattering centers
- $\langle \frac{d\sigma}{d\Omega} \rangle$ is the mean value of the differential cross section in a fixed energy interval
- $\Delta\Omega$ is the solid angle covered by the experimental set-up
- ε is the detection and software reconstruction efficiency
- B.R. is the branching ratio of the investigated decay mode

Tagged photon flux
The BGO-OD experiment will run at a photon flux of 10^7 γ/s in the tagged region 0.320-2.88 GeV.

For the estimation of the linearly polarised photon beam flux, simulation studies have been performed and the photon flux has been calculated for the optimization of the polarisation peak at several energies and considering photons with a polarisation degree greater than 30 %.

The calculated photon flux values usefull for the ω photoproduction measurements are listed in Tab.4, together with the corresponding energy range.

polarisation peak	flux [$10^7\gamma$ /s]	energy range [GeV]
unpolarised	0.438	1.10 - 2.88
at 1.2 GeV	0.39 $\cdot 10^{-1}$	1.10 - 1.33
at 1.4 GeV	0.80 $\cdot 10^{-1}$	1.13 - 1.50
at 1.6 GeV	0.52 $\cdot 10^{-1}$	1.38 - 1.67
at 1.7 GeV	0.38 $\cdot 10^{-1}$	1.53 - 1.76
at 1.8 GeV	0.25 $\cdot 10^{-1}$	1.68 - 1.84

Table 4 Photon flux

Number of scattering centers
The number of scattering centers is calculated according with the following formula:

$$N_{SC} = \frac{N_{Av}}{mw[g]} \cdot \frac{N_{p,n}}{molecule} \cdot \rho_{H_2(D_2)} \frac{[g]}{[cm]^3} \cdot tl[cm]$$

with mw being the mole weight and tl the target length. The results for proton (free proton in liquid H_2 target) and neutron (quasi free neutron in liquid D_2 target) are listed in Tab.5.

	N_{Av}	mw [g]	$N_{p,n}$/molecule	ρ [g]/[cm]^3	tl [cm]	N_{SC} particles/[cm]^2
H_2	$6.022 \cdot 10^{22}$	2	2	0.0678	6	$2.448 \cdot 10^{23}$
D_2	$6.022 \cdot 10^{22}$	4	2	0.169	6	$3.053 \cdot 10^{23}$

Table 5 Number of scattering centers

The estimation of the remaining terms of Eqn.1 has been performed by dedicated kinematical studies for each decay mode, both for the proton and for the neutron case.

Kinematical studies for the reaction $\gamma p \to \omega p$, with $\omega \to \pi^+\pi^0\pi^-$
Kinematical studies have been performed for the ω photoproduction off free proton. ω events have been generated from threshold up to 3.2 GeV of incoming photon beam energy. The photon energy distribution is given by the well known Bremmstrahlung spectrum (with its typical $1/E_\gamma$ dependence) convoluted with the experimental total cross section of the reaction itself. The ω is then generated according with its differential cross section (expressed in μb in the event generator). The three-pion decay is simulated assuming a phase space distribution for the decay products (at this step there is still no difference between π^+ and π^- and they will be called π_1 and π_2). The decay $\pi^0 \to \gamma_1\gamma_2$ is also implemented, with $\gamma_{1(2)}$ being the most (less) energetic decay photon. The kinematical distributions of the final state particles are shown in Fig.7.

The events which are interesting in terms of data analysis are classified according with the geometrical acceptance of the detector. Photons are considered only if detected in the BGO calorimeter (efficiency ε_γ = 89 %); charged particles can be detected in the BGO and in the forward region including both the MRPC and the forward spectrometer (efficiency $\varepsilon_{charged}$ = 70 %). The combinations which are considered useful for the future analysis are listed in Tab.6 together with their occurrence probability and the correspondent detector efficiency.

	BGO	forward	occurence (%)	efficiency (%)
a)	$\gamma_1\ \gamma_2$ P	$\pi_1\ \pi_2$	9.09	27.76
b)	$\gamma_1\ \gamma_2$	$\pi_1\ \pi_2$ P	1.54	27.76
c)	γ_1 P	$\pi_1\ \pi_2$	3.52	30.85
d)	γ_1	$\pi_1\ \pi_2$ P	0.39	30.85
e)	γ_2 P	$\pi_1\ \pi_2$	8.17	30.85
f)	γ_2	$\pi_1\ \pi_2$ P	0.49	30.85
g)	$\gamma_1\ \gamma_2$ P $\pi_{1(2)}$	$\pi_{2(1)}$	9.64	27.76
h)	$\gamma_1\ \gamma_2\ \pi_{1(2)}$	P $\pi_{2(1)}$	3.59	27.76
i)	$\gamma_1\ \gamma_2$ P $\pi_1\ \pi_2$		2.73	27.76
l)	$\gamma_1\ \gamma_2\ \pi_1\ \pi_2$	P	8.59	27.76

Table 6 Useful statistics for the future analysis of the reaction $\gamma p \to \omega p$, with $\omega \to \pi^+\pi^0\pi^-$

The overall contribution is obtained by multiplying the occurrence of each combination by the corresponding efficiency and summing up the results all over the combinations. This value must then be multiplied by 10^{-6} barn to include the order of magnitude of the differential cross section (which is expressed in μb in the event generator) and finally by the branching ratio of the decay channel (89.2%):

$$\langle \tfrac{d\sigma}{d\Omega} \rangle \Delta\Omega \cdot \varepsilon \cdot B.R. = 0.1215 \cdot 10^{-30} \text{ particles} \cdot [\text{cm}]^2.$$

The number of $\omega \to \pi^+\pi^0\pi^-$ events per second is calculated for the unpolarised beam and for the several optimizations of linearly polarised beam. Results are listed in Tab.7

polarisation peak	$E_{\vec{\gamma}}$ [GeV]	$N_{\vec{\gamma}}$/s ($\cdot 10^7$) particle $\cdot$ [s^{-1}]	N_{SC} particle $\cdot$ [cm^{-2}]	$\langle \frac{d\sigma}{d\Omega} \rangle \Delta\Omega \cdot \varepsilon \cdot B.R.$ [cm^2]	$N_{\omega\to\pi^+\pi^0\pi^-}$/s particle $\cdot$ [s^{-1}]
unpolarised	1.10 - 2.88	0.438	$2.448 \cdot 10^{23}$	$0.12 \cdot 10^{30}$	0.128
at 1.2 GeV	1.10 - 1.33	$0.39 \cdot 10^{-1}$	$2.448 \cdot 10^{23}$	$0.12 \cdot 10^{30}$	0.011
at 1.4 GeV	1.13 - 1.50	$0.80 \cdot 10^{-1}$	$2.448 \cdot 10^{23}$	$0.12 \cdot 10^{30}$	0.023
at 1.6 GeV	1.38 - 1.67	$0.52 \cdot 10^{-1}$	$2.448 \cdot 10^{23}$	$0.12 \cdot 10^{30}$	0.015
at 1.7 GeV	1.53 - 1.76	$0.38 \cdot 10^{-1}$	$2.448 \cdot 10^{23}$	$0.12 \cdot 10^{30}$	0.011
at 1.8 GeV	1.68 - 1.84	$0.25 \cdot 10^{-1}$	$2.448 \cdot 10^{23}$	$0.12 \cdot 10^{30}$	0.007

Table 7 Number of ω mesons per second off proton for the decay $\omega \to \pi^+\pi^0\pi^-$

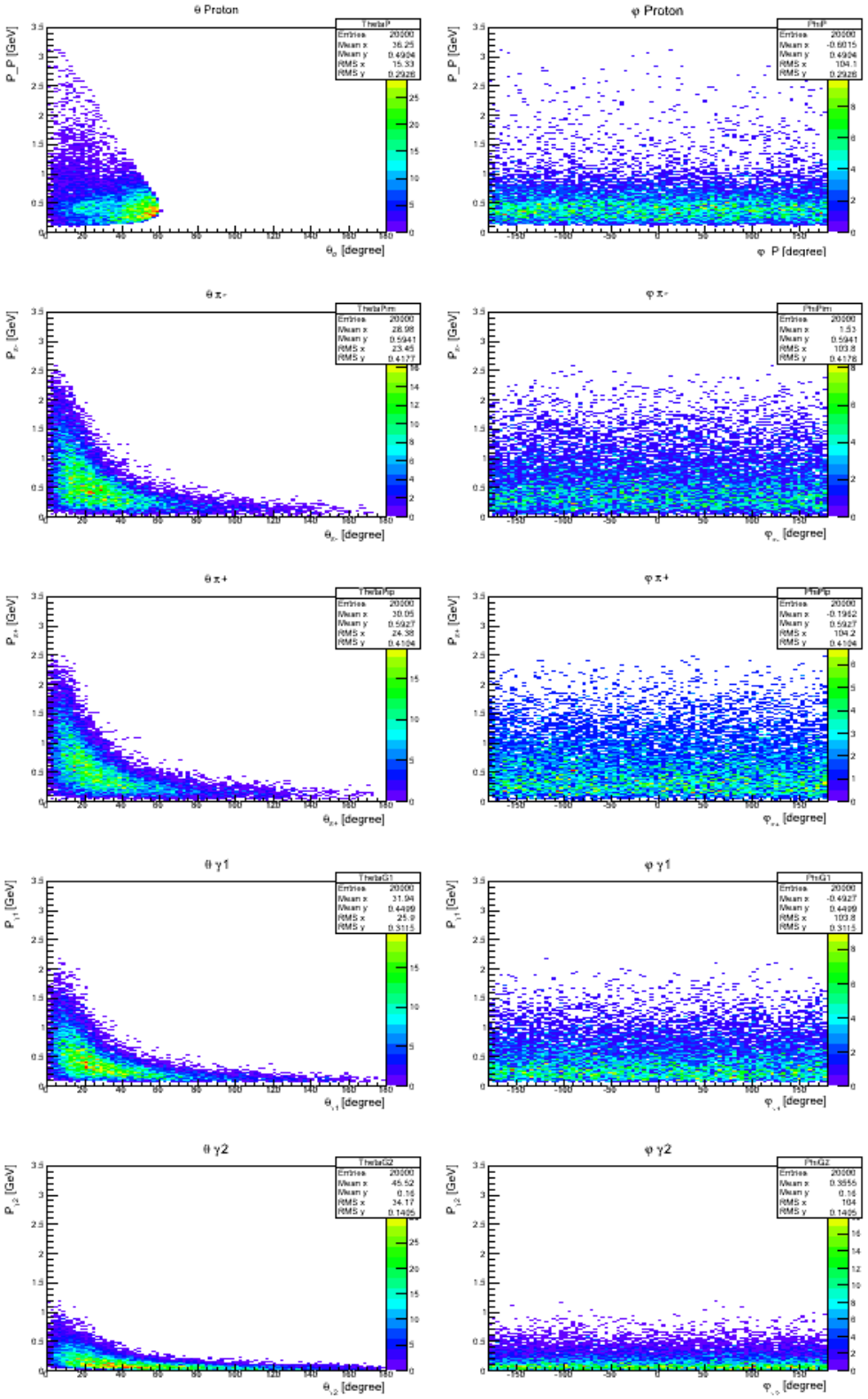

Figure 7 Kinematical distributions of the final state particles of the reaction $\gamma p \rightarrow \omega p$, with $\omega \rightarrow \pi^+\pi^0\pi^-$. For all the particles in the final state, the polar and azimuthal angle distributions are shown with respect to the momentum of the particle itself.

Kinematical studies for the reaction $\gamma p \to \omega p$, with $\omega \to \pi^0\gamma$
In analogy to what has been done for the three-pion decay, kinematical studies have been performed also for the radiative decay. The kinematical distributions of the final state particles are shown in Fig.8. Both the $\omega \to \pi^0\gamma$ decay and the $\pi^0 \to \gamma_1\gamma_2$ decay are generated by a phase space distribution. As before, for convention $\gamma_{1(2)}$ is the most (less) energetic photon from π^0 decay. The events which are considered useful for the future analysis are classified according with the geometrical acceptance of the detector and listed in Tab.8 together with their occurrence probability and the detector efficiency. The overall contribution is obtained by multiplying the occurrence of each combination by the corresponding efficiency and summing up the results all over the combinations. This value must then be multiplied by 10^{-6} barn to include the order of magnitude of the cross section (which is expressed in units of μb in the event generator) and finally by the branching ratio of the decay channel (8.28%):

$$\langle \tfrac{d\sigma}{d\Omega} \rangle \Delta\Omega \cdot \varepsilon \cdot B.R. = 0.0265 \cdot 10^{-30} \text{ particles} \cdot [\text{cm}]^2.$$

The number of $\omega \to \pi^0\gamma$ events per second is calculated for the unpolarised beam and for the several optimizations of linearly polarised beam. Results are listed in Tab.9.

	BGO	forward	occurrence (%)	efficiency (%)
a)	$\gamma\ \gamma_1\ \gamma_2$ P		7.31	50.96
b)	$\gamma\ \gamma_1\ \gamma_2$	P	11.46	50.96
c)	$\gamma\ \gamma_1$ P	γ_2	2.89	56.65
d)	$\gamma\ \gamma_1$	γ_2 P	2.23	56.65
e)	$\gamma\ \gamma_2$ P	γ_1	7.03	56.65
f)	$\gamma\ \gamma_2$	γ_1 P	2.72	56.65
g)	$\gamma_1\ \gamma_2$ P	γ	19.54	56.65
h)	$\gamma_1\ \gamma_2$	γ P	5.21	56.65

Table 8 Useful statistics for future analysis for the reaction $\gamma p \to \omega p$, with $\omega \to \pi^0\gamma$

polarisation peak	$E_{\vec{\gamma}}$ [GeV]	$N_{\vec{\gamma}}$/s ($\cdot 10^7$) particle $\cdot$ [s^{-1}]	N_{SC} particle $\cdot$ [cm^{-2}]	$\langle \frac{d\sigma}{d\Omega} \rangle \Delta\Omega \cdot \varepsilon \cdot B.R.$ [cm^2]	$N_{\omega\to\pi^0\gamma}$/s particle $\cdot$ [s^{-1}]
unpolarised	1.00 - 2.88	0.438	$2.448 \cdot 10^{23}$	$0.026 \cdot 10^{30}$	0.028
at 1.2 GeV	1.10 - 1.33	$0.39 \cdot 10^{-1}$	$2.448 \cdot 10^{23}$	$0.026 \cdot 10^{30}$	0.002
at 1.4 GeV	1.13 - 1.50	$0.80 \cdot 10^{-1}$	$2.448 \cdot 10^{23}$	$0.026 \cdot 10^{30}$	0.005
at 1.6 GeV	1.38 - 1.67	$0.52 \cdot 10^{-1}$	$2.448 \cdot 10^{23}$	$0.026 \cdot 10^{30}$	0.003
at 1.7 GeV	1.53 - 1.76	$0.38 \cdot 10^{-1}$	$2.448 \cdot 10^{23}$	$0.026 \cdot 10^{30}$	0.002
at 1.8 GeV	1.68 - 1.84	$0.25 \cdot 10^{-1}$	$2.448 \cdot 10^{23}$	$0.026 \cdot 10^{30}$	0.002

Table 9 Number of ω mesons per second off proton for the decay $\omega \to \pi^0\gamma$

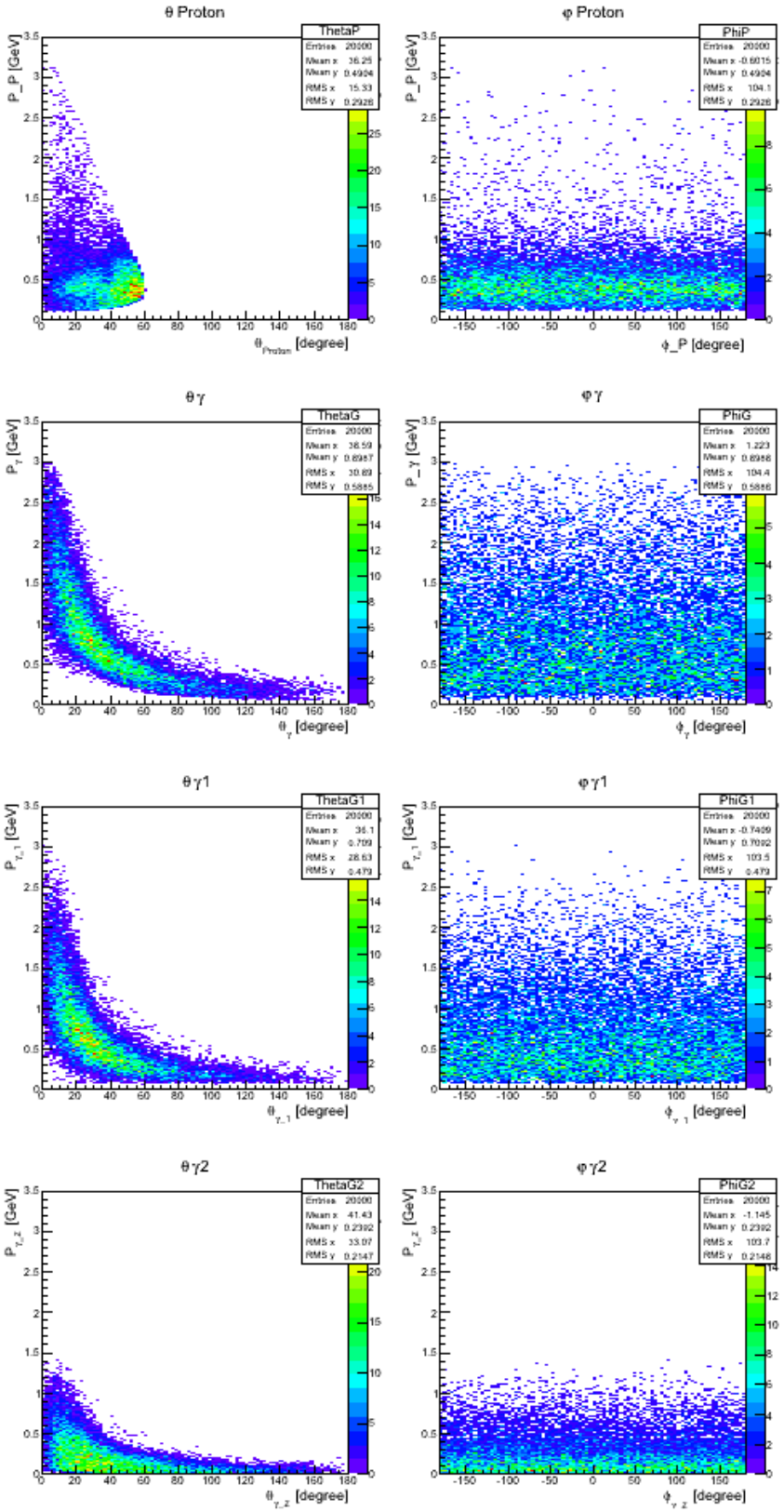

Figure 8 Kinematical distributions of the final state particles of the reaction $\gamma p \to \omega p$, with $\omega \to \pi^0\gamma$. For all the particles in the final state, the polar and azimuthal angle distributions are shown with respect to the momentum of the particle itself.

Kinematical studies for the reaction $\gamma n \to \omega n$, with $\omega \to \pi^+\pi^0\pi^-$
The same kinematical study has been performed also for the photoproduction off neutron, assuming the total and differential cross section being the same as for the photoproduction off proton. The neutron detection efficiency is ε_{BGO} = 40 % in the BGO calorimeter and ε_{FS} = 15% in the forward spectrometer (corresponding to the Time-of-Flight detector efficiency). The different combinations of final state particles which can be analysed are listed in Tab.10. The overall contribution is

$$\langle \tfrac{d\sigma}{d\Omega} \rangle \Delta\Omega \cdot \varepsilon \cdot B.R. = 0.053 \cdot 10^{-30} \text{ particles} \cdot [\text{cm}]^2.$$

The number of $\omega \to \pi^+\pi^0\pi^-$ events per second has been calculated for the unpolarised photon beam and for several optimisation of the linearly polarised photon beam. Results are listed in Tab.11.

	BGO	forward	occurrence (%)	efficiency (%)
a)	$\gamma_1\ \gamma_2$ N	$\pi_1\ \pi_2$	9.09	15.50
b)	$\gamma_1\ \gamma_2$	$\pi_1\ \pi_2$ N	0.17	5.80
c)	γ_1 N	$\pi_1\ \pi_2$	3.52	17.44
d)	γ_1	$\pi_1\ \pi_2$ N	0.05	6.54
e)	γ_2 N	$\pi_1\ \pi_2$	8.17	17.44
f)	γ_2	$\pi_1\ \pi_2$ N	0.08	6.54
g)	$\gamma_1\ \gamma_2$ N $\pi_{1(2)}$	$\pi_{2(1)}$	9.64	15.50
h)	$\gamma_1\ \gamma_2\ \pi_{1(2)}$	N $\pi_{2(1)}$	0.85	5.80
i)	$\gamma_1\ \gamma_2$ N $\pi_1\ \pi_2$		2.73	15.50
l)	$\gamma_1\ \gamma_2\ \pi_1\ \pi_2$	N	8.59	5.80

Table 10 Useful statistics for future analysis for the reaction $\gamma n \to \omega n$, with $\omega \to \pi^+\pi^0\pi^-$

polarisation peak	$E_{\vec{\gamma}}$ [GeV]	$N_{\vec{\gamma}}$/s ($\cdot 10^7$) particle $\cdot$ [s^{-1}]	N_{SC} particle $\cdot$ [cm^{-2}]	$\langle \frac{d\sigma}{d\Omega} \rangle \Delta\Omega \cdot \varepsilon \cdot B.R.$ [cm^2]	$N_{\omega\to\pi^+\pi^0\pi^-}$/s particle $\cdot$ [s^{-1}]
unpolarised	1.10 - 2.88	0.438	$3.053 \cdot 10^{23}$	$0.05 \cdot 10^{-30}$	0.067
at 1.2 GeV	1.10 - 1.33	$0.39 \cdot 10^{-1}$	$3.053 \cdot 10^{23}$	$0.05 \cdot 10^{-30}$	0.006
at 1.4 GeV	1.13 - 1.50	$0.80 \cdot 10^{-1}$	$3.053 \cdot 10^{23}$	$0.05 \cdot 10^{-30}$	0.013
at 1.6 GeV	1.38 - 1.67	$0.52 \cdot 10^{-1}$	$3.053 \cdot 10^{23}$	$0.05 \cdot 10^{-30}$	0.008
at 1.7 GeV	1.53 - 1.76	$0.38 \cdot 10^{-1}$	$3.053 \cdot 10^{23}$	$0.05 \cdot 10^{-30}$	0.006
at 1.8 GeV	1.68 - 1.84	$0.25 \cdot 10^{-1}$	$3.053 \cdot 10^{23}$	$0.05 \cdot 10^{-30}$	0.004

Table 11 Number of ω mesons per second off neutron for the decay $\omega \to \pi^+\pi^0\pi^-$

Kinematical studies for the reaction $\gamma n \to \omega n$, with $\omega \to \pi^0\gamma$
The same studies for the radiative decay give the following result:

$$\langle \tfrac{d\sigma}{d\Omega} \rangle \Delta\Omega \cdot \varepsilon \cdot B.R. = 0.009 \cdot 10^{-30} \text{ particles} \cdot [\text{cm}]^2.$$

The combination of final state particles which will be further included in the data analysis are listed in Tab.12. The number of $\omega \to \pi^0\gamma$ per second is calculated for the unpolarised photon beam and for the different polarisation settings. Results are listed in Tab.13.

	BGO	forward	occurence (%)	effciency (%)
a)	$\gamma\ \gamma_1\ \gamma_2$ N		7.315	28.19
b)	$\gamma\ \gamma_1\ \gamma_2$	N	1.92	10.57
c)	$\gamma\ \gamma_1$ N	γ_2	2.89	31.68
d)	$\gamma\ \gamma_1$	γ_2 N	0.37	11.88
e)	$\gamma\ \gamma_2$ N	γ_1	7.03	31.68
f)	$\gamma\ \gamma_2$	γ_1 N	0.34	11.88
g)	$\gamma_1\ \gamma_2$ N	γ	19.54	31.68
h)	$\gamma_1\ \gamma_2$	γ N	0.685	11.88

Table 12 Useful statistics for future analysis for the reaction $\gamma n \to \omega n$, with $\omega \to \pi^0\gamma$

polarisation peak	$E_{\vec{\gamma}}$ [GeV]	$N_{\vec{\gamma}}$/s ($\cdot 10^7$) particle $\cdot$ [s^{-1}]	N_{SC} particle $\cdot$ [cm^{-2}]	$\langle \frac{d\sigma}{d\Omega} \rangle \Delta\Omega \cdot \varepsilon \cdot B.R.$ [cm^2]	$N_{\omega\to\pi^0\gamma}$/s particle $\cdot$ [s^{-1}]
unpolarised	1.10 - 2.88	0.438	$3.053 \cdot 10^{23}$	$0.05 \cdot 10^{-30}$	0.0120
at 1.2 GeV	1.10 - 1.33	$0.39 \cdot 10^{-1}$	$3.053 \cdot 10^{23}$	$0.009 \cdot 10^{-30}$	0.0010
at 1.4 GeV	1.13 - 1.50	$0.80 \cdot 10^{-1}$	$3.053 \cdot 10^{23}$	$0.009 \cdot 10^{-30}$	0.0021
at 1.6 GeV	1.38 - 1.67	$0.52 \cdot 10^{-1}$	$3.053 \cdot 10^{23}$	$0.009 \cdot 10^{-30}$	0.0014
at 1.7 GeV	1.53 - 1.76	$0.38 \cdot 10^{-1}$	$3.053 \cdot 10^{23}$	$0.009 \cdot 10^{-30}$	0.0010
at 1.8 GeV	1.68 - 1.84	$0.25 \cdot 10^{-1}$	$3.053 \cdot 10^{23}$	$0.009 \cdot 10^{-30}$	0.0007

Table 13 Number of ω mesons off neutron for second for the decay $\omega \to \pi^0\gamma$

5.1 $\vec{\gamma}p \to \omega p$: beam asymmetry

For the calculation of the required beam hours, the following formula has been used:

$$\text{Time} = \varepsilon_r \frac{(N_\omega/bin)\cdot N_{bin}(E_{\vec{\gamma}})\cdot N_{bin}(\theta^*_\omega)}{(N_\omega/s)}$$

with ε_r = 0.5 being the total running efficiency given by the macroscopic duty cycle of the accelerator (0.71) times the trigger efficiency (0.75) times a safety margin factor (0.93).
It has been calculated that an uncertainty $\Delta\Sigma \approx 0.05$ can be achieved if 1000 ω events are collected for each $E_{\vec{\gamma}}$ and θ^*_ω bin.
The number of θ^*_ω bins is 5 for each $E_{\vec{\gamma}}$ bin. The number of $E_{\vec{\gamma}}$ bins is calculated in order to have 100 MeV width bin in the energy range $E_{\vec{\gamma}}$ = 1.1 - 1.5 GeV for comparison with already published results and 50 MeV in the new exploited energy range $E_{\vec{\gamma}}$ = 1.5 - 1.85 GeV. In Tab.14 the required beam hours are listed for each polarisation setting.

polarisation peak	$E_{\vec{\gamma}}$ [GeV]	$N_{bin}(E_{\vec{\gamma}})$	$N_{bin}(\theta^*_\omega)$	N_ω/s	hours
at 1.2 GeV	1.10 - 1.33	2	5	0.013	106
at 1.4 GeV	1.13 - 1.50	4	5	0.028	99
at 1.6 GeV	1.38 - 1.67	4	5	0.018	154
at 1.7 GeV	1.53 - 1.76	4	5	0.013	213
at 1.8 GeV	1.68 - 1.84	3	5	0.009	231
Total					**803**

Table 14 Minimum amount of beam hours for the measurement of Σ of the reaction $\vec{\gamma}p \to \omega p$.

The measurement of the Σ beam asymmetry off proton will run in parallel with the measurement of the spin density matrix elements (Sec.5.2).

5.2 $\vec{\gamma}p \to \omega p$: spin density matrix elements

The spin density matrix elements extraction will be performed only for the three-pion decay. For the calculation of the required beam hours, it must be taken into account that decay angular distributions must be studied both as a function of $\cos(\Theta)$ - for which 10 bins will be used - and as a function of $\cos(2\Phi)$ - for which 12 bins will be used. The beam time request is then dominated by the number of Φ bins. The $E_{\vec{\gamma}}$ bin width will be 100 MeV in the whole energy range. The last bin will have 140 MeV width (from 1.7 to 1.84 GeV) for time constraints.

$$\text{Time} = \varepsilon_r \frac{(N_\omega/bin)\cdot N_{bin}(E_{\vec{\gamma}})\cdot N_{bin}(\Phi)}{(N_\omega/s)}$$

In Tab.15 the required beam hours are listed for each polarisation setting.

polarisation peak	$E_{\vec{\gamma}}$ [GeV]	$N_{bin}(E_{\vec{\gamma}})$	$N_{bin}(\Phi)$	N_ω/s	hours
at 1.2 GeV	1.10 - 1.33	2	12	0.011	303
at 1.4 GeV	1.13 - 1.50	4	12	0.023	289
at 1.6 GeV	1.38 - 1.67	3	12	0.015	333
at 1.7 GeV	1.53 - 1.76	2	12	0.011	303
at 1.8 GeV	1.68 - 1.84	1	12	0.007	238
Total					**1466**

Table 15 Minimum amount of beam hours for the SDME extraction of the reaction $\vec{\gamma}p \to \omega p$.

5.3 $\gamma n \to \omega n$: differential cross section

For the calculation of the required beam hours, the following formula has been used:

$$\text{Time} = \varepsilon_r \frac{(N_\omega/bin)\cdot N_{bin}(E_\gamma)\cdot N_{bin}(\theta^*_\omega)}{(N_\omega/s)} = 0.5\frac{1000\cdot 17\cdot 10}{0.079} = 298 \text{ hours} \simeq \textbf{300 hours}.$$

The measurement of the differential cross section will be performed in 17 bins of E_γ (width $\simeq$ 100 MeV) and in 10 bins of θ^*_ω. The required number of ω events per bin is 1000.

The measurement of the differential cross section of ω photoproduction off neutron will run in parallel with the one for the ϕ photoproduction off neutron (Sec.6.3)

5.4 $\vec{\gamma} n \to \omega n$: beam asymmetry

For the beam asymmetry off neutron, the same number of bins as for the target proton case are required. In Tab.16, the minimum amount of necessary beam hours is listed for each polarization setting.

polarisation peak	$E_{\vec{\gamma}}$ [GeV]	$N_{bin}(E_{\vec{\gamma}})$	$N_{bin}(\theta^*_\omega)$	N_ω/s	hours
at 1.2 GeV	1.10 - 1.33	2	5	0.007	198
at 1.4 GeV	1.13 - 1.50	4	5	0.015	183
at 1.6 GeV	1.38 - 1.67	4	5	0.009	295
at 1.7 GeV	1.53 - 1.76	4	5	0.007	396
at 1.8 GeV	1.68 - 1.84	3	5	0.004	443
Total					**1515**

Table 16 Minimum amount of beam hours for the measurement of Σ of the reaction $\vec{\gamma} n \to \omega n$.

6 Request of beamtime: ϕ photoproduction

The estimation of the necessary beam hours requires the calculation of the number of ϕ mesons per second that we will be able to collect. As for the ω meson, this number is calculated according with the following formula:

$$\frac{N_\phi}{s} = \frac{N_\gamma}{s} \cdot N_{SC} \cdot \langle \frac{d\sigma}{d\Omega} \rangle \Delta\Omega \cdot \varepsilon \cdot B.R. \tag{2}$$

The discussion of the photon flux term (N_γ/s) and of the number of scattering centers (N_{SC}) has been performed already in page 12 and the corresponding values are listed in Tab.4 and 5, respectively. The flux of unpolarised photon is recalculated taking into account the threshold of the reaction $\gamma p \to \phi p$ (E_γ^{th} = 1.57 GeV): $N_\gamma/s = 0.276 \cdot 10^7 \gamma$/s.
The estimation of remaining terms in Eqn.2 has been performed on the basis of kinematical studies of the decay $\phi \to K^+K^-$ both off proton and off neutron target.

Kinematical studies for the reaction $\gamma p \to \phi p$, with $\phi \to K^+K^-$
As for the ω channel, kinematical studies have been performed from threshold up to 3.2 GeV of incoming photon beam energy. The photon energy distribution is given by the convolution of the incoherent Bremsstrahlung spectrum with the total cross section of the reaction itself. The ϕ meson is then generated according with its differential cross section (expressed in μb in the event generator). The decay into charged kaons is then generated assuming a phase space distribution of the decay particles. In this analysis K^+ and K^- can not be distinguished and will be called K_1 and K_2. In Fig.9 the kinematical distributions of the final state particles are shown.

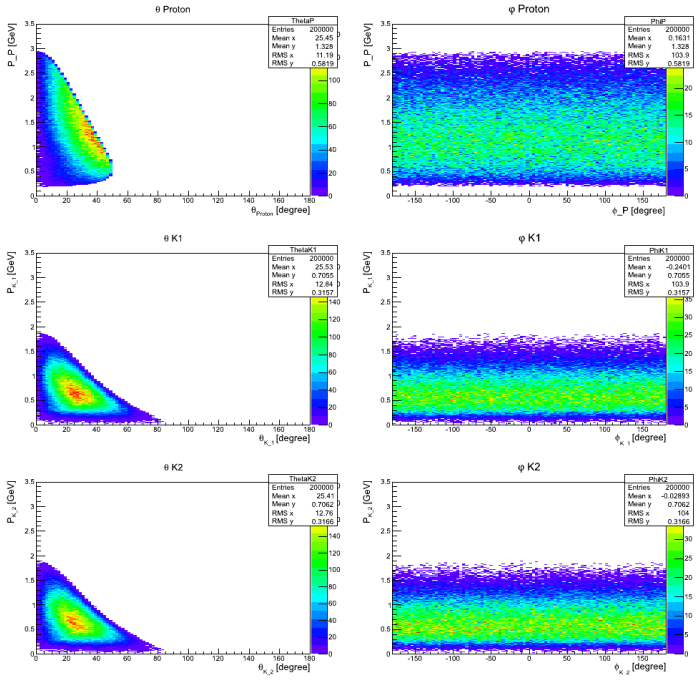

Figure 9 Kinematical distributions of the final state particles of the reaction $\gamma p \to \phi p$, with $\phi \to K_1K_2$. For all the three particles in the final state, the polar and azimuthal angle distributions are shown with respect to the momentum of the particle itself.

The events which are interesting in terms of future data analysis are classified according with the geometrical acceptance of the detector. They are listed in Tab.17 together with their occurrence probability and their efficiency (70 % for each charged particles; 34.30 % for the detection of all the three final state particles). The overall contribution is given by the sum of the occurrence of each combination times the efficiency. This value must then be multiplied by 10^{-6} barn to include the order of magnitude of

	BGO	forward	occurence (%)	effciency (%)
a)	P	$K_1\ K_2$	28.00	34.30
b)		P $K_1\ K_2$	5.80	34.30
c)	P $K_{1(2)}$	$K_{2(1)}$	18.45	34.30
d)	$K_{1(2)}$	P $K_{2(1)}$	18.79	34.30

Table 17 Useful statistics for future analysis for the reaction $\gamma p \to \phi p$, with $\phi \to K^+K^-$

the cross section (which is expressed in units of μb in the event generator) and finally by the branching ratio of the decay channel (48.9 %).

$$\langle \tfrac{d\sigma}{d\Omega} \rangle \Delta\Omega \cdot \varepsilon \cdot B.R. = 0.0119 \cdot 10^{-30} \text{ particles} \cdot [\text{cm}]^2.$$

The number of ϕ per second is calculated for the unpolarised photon beam and for the different polarisation settings. Results are listed in Tab.18.

polarisation peak	$E_{\vec{\gamma}}$ [GeV]	$N_{\vec{\gamma}}$/s ($\cdot 10^7$) particle $\cdot$ [s^{-1}]	N_{SC} particle $\cdot$ [cm^{-2}]	$\langle \frac{d\sigma}{d\Omega} \rangle \Delta\Omega \cdot \varepsilon \cdot B.R.$ [cm^2]	$N_{\phi \to K^+K^-}$/s particle $\cdot$ [s^{-1}]
unpolarised	1.57 - 2.88	0.276	$2.448 \cdot 10^{23}$	$0.0119 \cdot 10^{-30}$	0.0080
at 1.6 GeV	1.57 - 1.67	$0.20 \cdot 10^{-1}$	$2.448 \cdot 10^{23}$	$0.0119 \cdot 10^{-30}$	0.0058
at 1.7 GeV	1.53 - 1.76	$0.38 \cdot 10^{-1}$	$2.448 \cdot 10^{23}$	$0.0119 \cdot 10^{-30}$	0.0111
at 1.8 GeV	1.68 - 1.84	$0.25 \cdot 10^{-1}$	$2.448 \cdot 10^{23}$	$0.0119 \cdot 10^{-30}$	0.0072

Table 18 Number of ϕ mesons per second off proton.

Kinematical studies for the reaction $\gamma n \to \phi n$, with $\phi \to K^+K^-$
The same kinematical study has been performed also for the photoproduction off neutron, assuming the same total and differential cross sections as for the proton case. As for the ω channel, the neutron efficiency is 40% in the BGO calorimeter and 15% in the forward spectrometer. We remind that charged particles can be detected also in the MRPC in the forward direction. The contribution of the several final state particles combination is listed in Tab.19. The overall contribution is:

$$\langle \tfrac{d\sigma}{d\Omega} \rangle \Delta\Omega \cdot \varepsilon \cdot B.R. = 0.0046 \cdot 10^{-30} \text{ particles} \cdot [\text{cm}]^2.$$

	BGO	forward	occurence (%)	effciency (%)
a)	N	$K_1\ K_2$	28.00	19.60
b)		N $K_1\ K_2$	0.90	7.35
c)	N $K_{1(2)}$	$K_{2(1)}$	18.45	19.60
d)	$K_{1(2)}$	N $K_{2(1)}$	3.69	7.35

Table 19 Useful statistics for future analysis for the reaction $\gamma n \to \phi n$, with $\phi \to K^+K^-$

The number of ϕ per second is calculated for the unpolarised photon beam and for the different polarisation settings. Results are listed in Tab.20.

polarisation peak	$E_{\vec{\gamma}}$ [GeV]	$N\vec{\gamma}$/s particle $\cdot$ [s^{-1}]	N_{SC} particle $\cdot$ [cm^{-2}]	$\langle \frac{d\sigma}{d\Omega} \rangle \Delta\Omega \cdot \varepsilon \cdot B.R.$ [cm^2]	$N_{\phi \to K^+K^-}$/s particle $\cdot$ [s^{-1}]
unpolarised	1.57 - 2.88	0.276	$3.053 \cdot 10^{23}$	$0.0046 \cdot 10^{-30}$	0.0039
at 1.6 GeV	1.57 - 1.67	$0.20 \cdot 10^{-1}$	$3.053 \cdot 10^{23}$	$0.0046 \cdot 10^{-30}$	0.0003
at 1.7 GeV	1.53 - 1.76	$0.38 \cdot 10^{-1}$	$3.053 \cdot 10^{23}$	$0.0046 \cdot 10^{-30}$	0.0005
at 1.8 GeV	1.68 - 1.84	$0.25 \cdot 10^{-1}$	$3.053 \cdot 10^{23}$	$0.0046 \cdot 10^{-30}$	0.0003

Table 20 Number of ϕ mesons off neutron per second.

6.1 $\gamma p \to \phi p$: differential cross section

For the calculation of the required beam hours, the following formula has been used:

$$\text{Time} = \varepsilon_r \frac{(N_\phi/bin)\cdot N_{bin}(E_\gamma)\cdot N_{bin}(\theta^*_\phi)}{(N_\phi/s)} = 0.5\frac{500\cdot 13\cdot 4}{0.008} \simeq \textbf{452 hours}$$

In order to compare our results with the already published LEPS results at least 4 bins in θ^*_ϕ and 13 bins in $E_{\vec{\gamma}}$ are required (100 MeV width). The required number of ϕ events per bin is 500.

6.2 $\vec{\gamma} p \to \phi p$: beam asymmetry

The minimum amount of hours necessary for the measurement of Σ is given by the formula:

$$\text{Time} = \varepsilon_r \frac{(N_\phi/bin)\cdot N_{bin}(E_{\vec{\gamma}})\cdot N_{bin}(\theta^*_\phi)}{(N_\phi/s)}$$

At least 1000 events per bin are required for an uncertainty $\Delta\Sigma \approx 0.05$. The requires hours are listed in Tab.21 for the different polarisation settings.

polarisation peak	$E_{\vec{\gamma}}$ [GeV]	$N_{bin}(E_{\vec{\gamma}})$	$N_{bin}(\theta^*_\phi)$	N_ϕ/s	hours
at 1.7 GeV	1.57 - 1.76	4	5	0.0111	250
at 1.8 GeV	1.68 - 1.84	3	5	0.0072	298
Total					**548**

Table 21 Minimum amount of hours for the measurement of Σ of the reaction $\vec{\gamma} p \to \phi p$.

6.3 $\gamma n \to \phi n$: differential cross section

As in Sec.6.1 the calculation of the minimum amount of beam hours has been performed by using the following formula:

$$\text{Time} = \varepsilon_r \frac{(N_\phi/bin)\cdot N_{bin}(E_\gamma)\cdot N_{bin}(\theta^*_\phi)}{(N_\phi/s)}$$

If the same number of bins as for the target proton case are required (4 bins in θ^*_ϕ and 13 bins in $E_{\vec{\gamma}}$) the time request amounts to **952 hours**.

If this value exceeds the limit of the facility, the measurement of the differential cross section can be limited at the energy range E_γ = 1.57 - 2.3 GeV, covering at least the energy region corresponding to the bump structure observed for the target proton case. The number of energy bins can be reduced from 13 to 7 and the time request reduces to **500 hours**.

7 Conclusions

As a summary of the previous sections, in Tab.22 the minimum amount oh beam hours is listed again for each experiment.

Reaction	Observable	Beam polarisation	Hours
$\vec{\gamma}p \to \omega p$	Σ	at 1.2 GeV	**106**
		at 1.4 GeV	**99**
		at 1.6 GeV	**154**
		at 1.7 GeV	**213**
		at 1.8 GeV	**231**
	Total		$\simeq$ **803**
$\vec{\gamma}p \to \omega p$	SDME	at 1.2 GeV	**303**
		at 1.4 GeV	**289**
		at 1.6 GeV	**333**
		at 1.7 GeV	**303**
		at 1.8 GeV	**238**
	Total		$\simeq$ **1466**
$\gamma n \to \omega n$	$\frac{d\sigma}{dt}$	unpolarised	**300**
$\vec{\gamma}n \to \omega n$	Σ	at 1.2 GeV	**198**
		at 1.4 GeV	**183**
		at 1.6 GeV	**295**
		at 1.7 GeV	**396**
		at 1.8 GeV	**443**
	Total		$\simeq$ **1515**
$\gamma p \to \phi p$	$\frac{d\sigma}{dt}$	unpolarised	**452**
$\vec{\gamma}p \to \phi p$	Σ	at 1.7 GeV	**250**
		at 1.8 GeV	**298**
	Total		$\simeq$ **548**
$\gamma n \to \phi n$	$\frac{d\sigma}{dt}$	unpolarised	**952**

Table 22 Summary of the requested beam hours

Several parts of the sub-proposals have strong overlaps in terms of beam hours and polarisation optimisation. In Tab.23 all the overlapping sub-proposals have been merged in order to formulate the definitive beam hours request. The properties of the electron and of photon beam are listed; the required taget is mentioned; the total amount of hours is request and (in the last column) the corresponding sub-proposals are listed.

ELSA beam	**Photon Beam**	**Target**	**hours**	**Measurement**
E_{e^-} = 3.2 GeV, unpolarised	unpolarised	H_2	**500**	$\frac{d\sigma}{dt}$ for $\gamma p \to \phi p$
E_{e^-} = 3.2 GeV, unpolarised	polarised at 1.2 GeV	H_2	**350**	Σ for $\vec{\gamma} p \to \omega p$ SDME for $\vec{\gamma} p \to \omega p$
E_{e^-} = 3.2 GeV, unpolarised	polarised at 1.6 GeV	H_2	**350**	Σ for $\vec{\gamma} p \to \omega p$ SDME for $\vec{\gamma} p \to \omega p$
E_{e^-} = 3.2 GeV, unpolarised	polarised at 1.7 GeV	H_2	**250**	Σ for $\vec{\gamma} p \to \phi p$
E_{e^-} = 3.2 GeV, unpolarised	polarised at 1.8 GeV	H_2	**300**	Σ for $\vec{\gamma} p \to \omega p$ SDME for $\vec{\gamma} p \to \omega p$ Σ for $\vec{\gamma} p \to \phi p$
E_{e^-} = 3.2 GeV, unpolarised	unpolarised	D_2	**1000**	$\frac{d\sigma}{dt}$ for $\gamma n \to \omega n$ $\frac{d\sigma}{dt}$ for $\gamma n \to \phi n$
E_{e^-} = 3.2 GeV, unpolarised	polarised at 1.2 GeV	D_2	**250**	Σ for $\vec{\gamma} n \to \omega n$
E_{e^-} = 3.2 GeV, unpolarised	polarised at 1.6 GeV	D_2	**350**	Σ for $\vec{\gamma} n \to \omega n$
E_{e^-} = 3.2 GeV, unpolarised	polarised at 1.8 GeV	D_2	**450**	Σ for $\vec{\gamma} n \to \omega n$

Table 23 Final beam hours request

8 References

[1] J.Beringer *et al.*, Phys. Rev. D **8**6, 010001 (2012), URL: http://pdg.lbl.gov

[2] ABBHHM Coll., Phys. Rev. **1**75, 5 (1968)

[3] Y.Eisenberg *et al.*, Phys. Rev. Lett **22**, 13 (1969)

[4] J.Ballam *et al.*, Phys. Rev. D **7**, 11 (1973)

[5] F.J.Klein PiN Newslett. **14**, 141 (1998)

[6] J.Barth *et al.*, EPJ A **1**8, 117 (2003)

[7] J.Barth *et al.*, EPJ A **1**7, 269 (2003)

[8] Y.Oh *et al.*, Phys. Rev. C **6**3, 025201 (2001)

[9] M.Williams *et al.*, Phys. Rev. C **8**0, 065208 (2009)

[10] M.Williams *et al.*, Phys. Rev. C **8**0, 065209 (2009)

[11] A.Ajaka *et al.*, Phys. Rev. Lett. **9**6, 132003 (2006)

[12] F.Klein *et al.*, Phys. Rev. D **7**8, 117101 (2008)

[13] G.Penner and U.Mosel, Phys. Rev. C **6**6, 055212 (2002)

[14] V. Shklyar *et al.*, Phys. Rev. C **7**1, 055206 (2005)

[15] Q.Zhao *et al.*, Phys. Rev. C **7**1, 054004 (2005)

[16] M.Paris Phys. Rev. C **7**9, 025208 (2009)

[17] Contribution to NRNN09, V.Vegna *et al.*, Int. J. Mod. Phys. E **1**9, 1241 (2010)

[18] T.Mibe *et al.*, Phys. Rev. Lett. **9**5, 182001 (2005)

[19] A.I.Titov and T.-S.H.Lee, Phys. Rev. C **67**, 06205 (2003)

[20] A.Kiswandhi *et al.*, Phys. Lett. B **6**91, 214-218 (2010)

[21] O.Bartalini et al., Eur.Phys.J. A26 (2005) 399-419

[22] P. Levi Sandri et al., Nucl. Instrum. Methods Phys. Res. A 370 (1996) 396-402

[23] F. Ghio et al., Nucl. Instrum. Methods Phys. Res. A 404, (1998) 71-86

[24] M. Castoldi et al., Nucl. Instrum. Methods Phys. Res. A 403,(1998) 22-30